

Numerical study of surface-induced reorientation and smectic layering in a nematic liquid crystal

Joachim Stelzer*

Schwetzingen Str. 20, 69190 Walldorf (Baden), Germany

Ralf Bernhard

IMPACT Messtechnik, 71332 Waiblingen, Germany

Abstract

Surface-induced profiles of both nematic and smectic order parameters in a nematic liquid crystal, ranging from an orienting substrate to “infinity”, were evaluated numerically on base of an extended Landau theory. In order to obtain a smooth behavior of the solutions at “infinity” a boundary energy functional was derived by linearizing the Landau energy around its equilibrium solutions. We find that the intrinsic wave number of the smectic structure, which plays the rôle of a coupling between nematic and smectic order, strongly influences the director reorientation. Whereas the smectic order is rapidly decaying when moving away from the surface, the uniaxial nematic order parameter shows an oscillatory behavior close to the substrate, accompanied by a non-zero local biaxiality.

PACS numbers: 61.30.-v, 61.30.Cz, 64.70.Md

*Electronic address: js69190@gmx.de

I. INTRODUCTION

The structure of uniaxial nematic liquid crystals is strongly influenced by the presence of orienting surfaces [1]. In addition to the usual elastic distortions in the nematic bulk, which are well described by the Oseen-Zöcher-Frank energy, strong deformations can occur close to the surface substrate [2, 3]. These effects are often accompanied by a non-zero local biaxiality of the orientational order [4]. The nematic orientation close to a confining substrate could be detected experimentally using second-harmonic generation techniques [5]. In addition, by X-ray studies the surface has also been proven to induce a layered structure, *i.e.*, smectic order appears close to the surface which decays when moving away from the substrate into the nematic bulk [6]. In spite of considerable effort, both in theory [7, 8, 9, 10] and computer simulation [11, 12, 13, 14], the full complexity of surface-induced structural changes in nematics is far from being understood. Whereas Monte Carlo or molecular dynamics simulations approach the problem on the molecular level, in our contribution we take a phenomenological viewpoint. To this aim we consider an extended Landau theory, comparable to Skačej *et al.* [8]. In addition to that paper, we investigate not only uniaxial order, instead, both the full alignment tensor for nematic order and, mainly, the amplitude of the smectic layering is taken into account. In particular, the influence of the coupling between smectic and nematic order on the order parameter profiles, obtained from numerical relaxation, is investigated in detail. Whereas the boundary conditions at the surface substrate are fixed, an additional boundary energy is derived, in order to guarantee a smooth behavior of the profiles at “infinity” (far from the surface) where the volume equilibrium values of the order parameters should be reached.

The organization of the article is as follows. In Section II the Landau theory used in our calculations is introduced. We focus on the derivation of the additional boundary energy at “infinity” in the Appendix. Section III indicates the numerical relaxation method employed and presents selected results for order parameter profiles. Finally, Section IV contains some concluding remarks.

II. EXTENDED LANDAU THEORY FOR SURFACE-INDUCED EFFECTS

The geometry of our system is the semi-infinite space ($z \geq 0$), confined by a substrate surface at $z = 0$ and “infinity” ($z = \infty$) which, in numerical practice, means a large distance from the surface. Due to the infinite extension of the system in x and y direction and the absence of any lateral structure of the surface, we can reduce the problem to a one-dimensional geometry, *i.e.*, all quantities only depend on the distance z from the surface. In order to be able to investigate both positional and orientational order, we need two different order parameters. The smectic order parameter usually is a complex number, $\rho = \psi e^{i\chi}$, whose phase χ accounts for local layer deformations. We assume perfect layering at the surface ($\rho(z = 0) = 1$) and, therefore, we are left only with the amplitude $\psi(z)$ of the layering which is a real quantity indicating the degree of smectic order. The nematic order parameter is a second-rank traceless and symmetric tensor. Without loss of generality we choose its parametrization as

$$\mathbf{Q}(z) = \begin{pmatrix} Q_{xx}(z) & Q_{xy}(z) & Q_{xz}(z) \\ Q_{xy}(z) & Q_{yy}(z) & Q_{yz}(z) \\ Q_{xz}(z) & Q_{yz}(z) & -Q_{xx}(z) - Q_{yy}(z) \end{pmatrix}. \quad (1)$$

Therefore, there are six scalar functions whose profiles (z dependence) have to be determined. These profiles are found from a numerical minimization of an energy, supplied with appropriate boundary conditions at $z = 0$ and $z = \infty$.

A. Bulk energy functional

The bulk energy functional is chosen according to an extended Landau theory. It consists of a smectic and a nematic contribution. The smectic energy contains a volume and an elastic contribution [15],

$$\mathcal{F}_{\text{smec}} = \frac{1}{2} \tau |\rho|^2 + |\rho|^4 + \frac{1}{2} \kappa |(\nabla - i q_0 \delta \mathbf{n}_\perp) \rho|^2. \quad (2)$$

Due to the continuity of the smectic-nematic phase transition, the volume smectic energy is an expansion into even powers of the smectic order parameter ρ . This phase transition occurs at $\tau = 0$, where τ is a reduced temperature. The last expression in (2) is the elastic energy due to the gradients of the layer amplitude (with smectic elastic constant κ). It incorporates

a *coupling to the nematic order*, based on local $U(1)$ gauge invariance, due to the nature of the smectic order parameter as a complex number [15]. Namely, local changes of the smectic order are accompanied by transversal fluctuations of the director field \mathbf{n} , perpendicular to the layer normal. In our simplified geometry these fluctuations are always in the x - y plane. The coupling strength is given by the intrinsic wave number q_0 of the smectic layering. After inserting the nematic tensor order parameter (1) and reducing the smectic order parameter to its amplitude, the smectic energy becomes a functional dependent on $\psi(z)$, ψ' (prime denoting derivative with respect to z) and $Q_{ij}(z)$,

$$\mathcal{F}_{\text{smec}} = \frac{1}{2} \tau \psi^2 + \psi^4 + \frac{1}{2} \kappa \left[\psi'^2 + q_0^2 \left(Q_{xx} + Q_{yy} + \frac{2}{3} S_{\text{vol}} \right) \psi^2 \right]. \quad (3)$$

Here, S_{vol} is the scalar order parameter that minimizes the volume *nematic* energy (see next subsection).

The nematic energy functional also consists of a volume and an elastic part,

$$\mathcal{F}_{\text{nem}} = \frac{1}{4} t Q_{ij} Q_{ji} - \sqrt{6} Q_{ij} Q_{jk} Q_{ki} + (Q_{ij} Q_{ji})^2 \quad (4)$$

$$+ \frac{1}{4} (\partial_i Q_{jk}) (\partial_i Q_{jk}) + \frac{1}{4} k_{21} (\partial_i Q_{ik}) (\partial_j Q_{jk}) + \frac{1}{4} k_{31} (\partial_k Q_{ij}) (\partial_j Q_{ik})$$

$$= \frac{1}{2} t (Q_{xx}^2 + Q_{xy}^2 + Q_{xz}^2 + Q_{yy}^2 + Q_{yz}^2 + Q_{xx} Q_{yy}) \quad (5)$$

$$- 3 \sqrt{6} (Q_{xx} Q_{xy}^2 + Q_{yy} Q_{xy}^2 - Q_{xx} Q_{yy}^2 - Q_{yy} Q_{xx}^2$$

$$- Q_{xx} Q_{yz}^2 - Q_{yy} Q_{xz}^2 + 2 Q_{xy} Q_{xz} Q_{yz})$$

$$+ 4 (Q_{xx}^2 + Q_{xy}^2 + Q_{xz}^2 + Q_{yy}^2 + Q_{yz}^2 + Q_{xx} Q_{yy})^2$$

$$+ \frac{1}{2} (Q'_{xx}^2 + Q'_{xy}^2 + Q'_{xz}^2 + Q'_{yy}^2 + Q'_{yz}^2 + Q'_{xx} Q'_{yy})$$

$$+ \frac{1}{4} (k_{21} + k_{31}) \cdot (Q'_{xx}^2 + Q'_{yy}^2 + Q'_{xz}^2 + Q'_{yz}^2 + 2 Q'_{xx} Q'_{yy}).$$

Unlike the smectic energy, the volume part of (4) contains a third-order expression, to describe the discontinuous isotropic-nematic phase transition, which, in our parametrization, occurs at $t = \frac{9}{8}$. (t is again a reduced temperature.) For the elastic part of (4) there are three independent deformation modes, similar to the Oseen-Zöcher-Frank theory for elastic distortions of the director. k_{21} and k_{31} denote the ratios of elastic constants for the respective deformation modes.

B. Boundary conditions

At the substrate surface the values for the order parameters are fixed. We assume ideal smectic and uniaxial nematic order. That means the smectic amplitude is one, and the alignment tensor is completely determined by the uniaxial scalar order parameter $S = 1$ and the fixed director surface tilt angle Θ_{surf} (measured in the x - z plane, from the z axis). This results in the Dirichlet boundary conditions,

$$\psi(z = 0) = 1 , \quad (6)$$

$$\mathbf{Q}(z = 0) = S \left(\mathbf{n} \otimes \mathbf{n} - \frac{1}{3} \mathbf{1} \right) \quad (7)$$

$$= \begin{pmatrix} \sin^2 \Theta_{\text{surf}} - \frac{1}{3} & 0 & \sin \Theta_{\text{surf}} \cos \Theta_{\text{surf}} \\ 0 & -\frac{1}{3} & 0 \\ \sin \Theta_{\text{surf}} \cos \Theta_{\text{surf}} & 0 & \cos^2 \Theta_{\text{surf}} - \frac{1}{3} \end{pmatrix} \quad (8)$$

At infinity, the boundary conditions are not of Dirichlet-type. Instead, we have to guarantee smooth profiles (zero slope) for the order parameters which should reach those values that minimize the *volume* parts of the smectic and nematic energy (3) and (5). To this aim we insert the uniaxial form of the alignment tensor (7) into (5). A direct minimization yields the temperature dependence of the volume order parameters,

$$\psi_{\text{vol}}(\tau) = \frac{1}{2} \sqrt{-\tau} , \quad (9)$$

$$S_{\text{vol}}(t) = \frac{6\sqrt{6} + \sqrt{216 - 192t}}{32} \quad (10)$$

The tilt angle to be reached at infinity is arbitrary. We take $\Theta = 0$, *i.e.*, director orientation along the surface normal, in accordance with previous molecular dynamics simulations [12].

Next we have to establish a boundary energy functional \mathcal{F}_∞ whose minimization leads to the desired surface profiles at infinity. Based upon the procedure introduced by Galatola *et al.* [16] the central idea for finding the boundary energy functional is a *linearization of the bulk equations around the volume order parameters* calculated above. We provide all details of this derivation, which is an important ingredient of our method, in the Appendix. Here

we merely quote the result,

$$\begin{aligned}\mathcal{F}_\infty = & \frac{1}{2} U (Q_{xx}^2 + Q_{yy}^2) + \frac{1}{3} (U + V) S_{\text{vol}} (Q_{xx} + Q_{yy}) \\ & + V Q_{xx} Q_{yy} + \frac{1}{2} \sqrt{G_{33}} \cdot Q_{xy}^2 \\ & + \frac{1}{2} \sqrt{\frac{1}{2} (2 + k_{21} + k_{31}) G_{44} \cdot (Q_{xz}^2 + Q_{yz}^2)} \\ & + \frac{1}{2} \sqrt{\kappa \tau} \cdot \psi^2 ,\end{aligned}\quad (11)$$

where U , V , G_{33} , G_{44} are terms which depend on the reduced temperatures τ and t , the nematic elastic constants k_{21} , k_{31} and the volume order parameter $S_{\text{vol}}(t)$. (For the explicit expressions see Appendix A.)

Now all order parameter profiles can be obtained from a minimization of the total energy

$$F = \int_0^\infty (\mathcal{F} + \mathcal{F}_\infty \delta(\infty)) dz , \quad (12)$$

with the Dirichlet boundary conditions (6) and (8) valid at $z = 0$.

III. ORDER PARAMETER PROFILES

The minimization of the total energy (12) was performed numerically, employing a standard Newton-Gauß-Seidel technique which, in our case, formally corresponds to a one-dimensional version of the Finite Element method. First the “infinite” distance from the surface was replaced by a large, finite value $z_{\text{max}} = 100$. The range $0 \leq z \leq z_{\text{max}}$ was discretized in $N = 1000$ intervals. The bulk and boundary energy functionals (3), (5), (11) were evaluated on these intervals, the derivatives with respect to z being replaced by finite differences. The values of the order parameters at $z = 0$ were fixed according to (6) and (8). For the initial configuration we assumed linear profiles for all quantities ψ and Q_{ij} on the interval $0 \leq z \leq z_{\text{max}}$, by interpolating between their surface and volume values. An iterative procedure was then performed on each grid point. All order parameters were corrected according to the Newton-Gauß-Seidel prescription,

$$X^{\text{new}} = X^{\text{old}} - \frac{\partial F / \partial X}{\partial^2 F / \partial X^2} , \quad (X = \psi, Q_{ij}) , \quad (13)$$

where the functional derivatives in (13) were evaluated by numerical differentiation. The relaxation was terminated when the relative change of the total energy was less than 10^{-6} which corresponded to some thousand relaxation steps.

For further discussion the nematic tensor order parameter will be analyzed in terms of its eigenvalues and eigenvectors. More specifically, we will plot the tilt angle of the main director, measured from the z axis and two scalar order parameters. The latter ones measure the degree of uniaxial and biaxial order, respectively. (We checked that the director twist angle stays constant, due to the surface anchoring in the x - z plane.)

The equilibrium profiles were evaluated for different values of the reduced temperature $t = 0\dots 1$ and the intrinsic smectic wave number $q_0 = 0.3\dots 0.8$. All other parameters were fixed. In particular, the elastic constants were chosen as $k_{21} = k_{31} = 1$ and $\kappa = 5$ which accounts for the fact that layer distortions should contain a higher elastic energy than deformations of orientational order. The reduced temperature was $\tau = 0.1$ which corresponds to a nematic state point, slightly above the smectic-nematic phase transition. Finally, the director at the surface was anchored at a tilt angle of $\Theta_{\text{surf}} = 60^\circ$.

Figures 1-3 correspond to a reduced temperature of $t = 0.0$ which means a nematic state point far away from the nematic-isotropic phase transition. The smectic order parameter profile is given in Fig. 1 for wave numbers $q_0 = 0.3, 0.6, 0.8$, corresponding to a layer spacing of 20.9, 12.6, 7.8. Obviously, the smectic structure is rapidly decaying from its maximum value of one when moving away from the surface. At a distance of 20 the curves essentially have reached their asymptotic value which, due to the finite size of our system, is not precisely at zero. This loss of smectic order is almost independent of the wave number.

As shown in Figure 2 the uniaxial nematic order parameter is also approaching its asymptotic value within a distance of 20. The value reached is 0.92, which precisely corresponds to the volume value of the scalar order parameter at temperature $t = 0.0$, according to (10). Remarkably, the uniaxial order parameter is not decaying monotonically, instead there is an oscillatory behavior. For large wave numbers ($q \geq 0.6$) it even decreases below its volume value. The non-monotonic behavior of uniaxial order is accompanied by the occurrence of a non-zero biaxial order parameter. Both suppression of uniaxial order and increased biaxiality close to the surface have also been observed in computer simulations based on the molecular Gay-Berne model [12].

Unlike the scalar order parameters, the profile of the director tilt angle strongly depends on the intrinsic smectic wave number (Figure 3). Whereas for $q_0 = 0.8$ there is again a strong change within a comparably short distance, for low wave numbers ($q \leq 0.6$) the director reorientation extends over the complete spatial range of 100. (The finite size effect is again

the reason for the non-zero tilt angle at distance 100.) The behavior of the tilt angle is also changing qualitatively with the wave number. *E.g.*, for $q_0 = 0.3$ the curvature is not unique any more, instead, the curve consists of convex and concave parts. As revealed from Figure 4, an even more drastic change occurs for the reduced temperature $t = 1.0$, which is just below the nematic-isotropic phase transition. For low wave numbers the tilt angle profiles show a local maximum at a distance of around 20, before decaying towards the volume value.

The influence of the smectic wave number on the director tilt angle profile can be understood from the particular form of the coupling energy (2). In order to minimize this coupling the transversal director components should be small in those regions where the smectic order parameter is significantly non-zero, *i.e.*, close to the surface. Therefore, it is obvious that for increasing wave number the reorientation of the tilt angle towards the direction of the surface normal becomes more pronounced. — Finally, all profiles reach their respective asymptotic values with (almost) zero slope indeed, which is due to the boundary energy functional that we have derived in the previous section.

IV. REMARKS

1. Summarizing our work, we have numerically analyzed the surface-induced profiles of smectic and nematic order as well as director orientation. Whereas the order parameters are always strongly changing in a thin layer close to the surface, the tilt angle reorientation is dependent on the intrinsic smectic wave number of the liquid crystal which, in our model, acts as a coupling parameter between nematic and smectic order. It seems, however, that the case of high wave number ($q = 0.8$) is the most realistic, considering the experimental observation of a strong reorientation close to the surface [5]. In addition, surface-induced biaxiality and suppression of uniaxial order, previously detected in experiment and molecular simulations, could also be confirmed within the frame of our model.
2. The asymptotic behavior of the profiles at infinity was reproduced in numerics by deriving a boundary energy functional. To this aim, referring to the method of Ref. [16] we linearized the bulk Euler-Lagrange equations around their volume solutions. When the boundary energy is included into the numerical minimization procedure, the order parameter profiles at infinity smoothly reach their volume values. Although in our

case this technique was used in a one-dimensional geometry, it could be extended in a straightforward way to more complex situations. For instance, a laterally structured surface, which is fairly common in novel developments of display technique, will already break the symmetry of our example. However, the treatment of open boundaries by an additional energy functional derived from a linearization of the bulk energy is a very general concept which could be used for any numerical study dealing with “infinitely” extended systems.

APPENDIX A: DERIVATION OF THE BOUNDARY ENERGY FUNCTIONAL

Before starting to derive the boundary energy functional at infinity, we first remind of the desired values for the order parameters. At infinity the smectic order is completely lost ($\psi(z = \infty) = 0$). The nematic order parameter is again uniaxial, but with the volume scalar order parameter $S_{\text{vol}}(t)$, dependent on temperature, and zero tilt angle,

$$\psi(z = \infty) = 0 \quad (\text{A1})$$

$$\begin{aligned} \mathbf{Q}(z = \infty) &= S \left(\mathbf{n} \otimes \mathbf{n} - \frac{1}{3} \mathbf{1} \right) \\ &= \begin{pmatrix} -\frac{1}{3} S_{\text{vol}}(t) & 0 & 0 \\ 0 & -\frac{1}{3} S_{\text{vol}}(t) & 0 \\ 0 & 0 & \frac{2}{3} S_{\text{vol}}(t) \end{pmatrix} \end{aligned} \quad (\text{A2})$$

We start with the bulk equation which are obtained from the bulk energy functional $\mathcal{F} = \mathcal{F}_{\text{smec}} + \mathcal{F}_{\text{nem}}$, (3) and (5), by variational calculus as the corresponding Euler-Lagrange equations,

$$L_X = \frac{\partial \mathcal{F}}{\partial X} - \frac{d}{dz} \frac{\partial \mathcal{F}}{\partial X'} = 0 \quad , \quad (X = \psi, Q_{ij}). \quad (\text{A3})$$

In order to obtain a smooth behavior of the profiles at infinity, the Euler-Lagrange equations (A3) are linearized around the volume order parameters. To that aim we calculate the partial

derivatives of the right-hand sides at infinity,

$$G_{11} = \left. \frac{\partial L_{xx}}{\partial Q_{xx}} \right|_{z=\infty} = \left. \frac{\partial L_{yy}}{\partial Q_{yy}} \right|_{z=\infty} = t - 2\sqrt{6} S_{\text{vol}} + \frac{40}{3} S_{\text{vol}}^2 , \quad (\text{A4})$$

$$G_{12} = \left. \frac{\partial L_{xx}}{\partial Q_{yy}} \right|_{z=\infty} = \left. \frac{\partial L_{yy}}{\partial Q_{xx}} \right|_{z=\infty} = \frac{1}{2} t - 4\sqrt{6} S_{\text{vol}} + \frac{32}{3} S_{\text{vol}}^2 , \quad (\text{A5})$$

$$G_{33} = \left. \frac{\partial L_{xy}}{\partial Q_{xy}} \right|_{z=\infty} = t + 4\sqrt{6} S_{\text{vol}} + \frac{16}{3} S_{\text{vol}}^2 , \quad (\text{A6})$$

$$G_{44} = \left. \frac{\partial L_{xz}}{\partial Q_{xz}} \right|_{z=\infty} = \left. \frac{\partial L_{yz}}{\partial Q_{yz}} \right|_{z=\infty} = t - 2\sqrt{6} S_{\text{vol}} + \frac{16}{3} S_{\text{vol}}^2 , \quad (\text{A7})$$

$$G_{66} = \left. \frac{\partial L_\psi}{\partial \psi} \right|_{z=\infty} = \tau . \quad (\text{A8})$$

The linearized Euler-Lagrange equations now become explicitly

$$Q''_{xx} = \frac{2}{3 + 2(k_{21} + k_{31})} \left[(2 + k_{21} + k_{31}) G_{11} - (1 + k_{21} + k_{31}) G_{12} \right] \left(Q_{xx} + \frac{1}{3} S_{\text{vol}} \right) \quad (\text{A9})$$

$$+ \frac{2}{3 + 2(k_{21} + k_{31})} \left[(2 + k_{21} + k_{31}) G_{12} - (1 + k_{21} + k_{31}) G_{11} \right] \left(Q_{yy} + \frac{1}{3} S_{\text{vol}} \right) ,$$

$$Q''_{yy} = \frac{2}{3 + 2(k_{21} + k_{31})} \left[-(1 + k_{21} + k_{31}) G_{11} + (2 + k_{21} + k_{31}) G_{12} \right] \left(Q_{xx} + \frac{1}{3} S_{\text{vol}} \right) \quad (\text{A10})$$

$$+ \frac{2}{3 + 2(k_{21} + k_{31})} \left[-(1 + k_{21} + k_{31}) G_{12} + (2 + k_{21} + k_{31}) G_{11} \right] \left(Q_{yy} + \frac{1}{3} S_{\text{vol}} \right) ,$$

$$Q''_{xy} = G_{33} Q_{xy} , \quad (\text{A11})$$

$$Q''_{xz} = \frac{2}{2 + k_{21} + k_{31}} G_{44} Q_{xz} , \quad (\text{A12})$$

$$Q''_{yz} = \frac{2}{2 + k_{21} + k_{31}} G_{44} Q_{yz} , \quad (\text{A13})$$

$$\psi'' = \frac{\tau}{\kappa} \psi . \quad (\text{A14})$$

Among the equations (A9)–(A14), the first two are coupled. In order to find their solutions we note that they can be written in matrix form,

$$\begin{pmatrix} Q''_{xx} \\ Q''_{yy} \end{pmatrix} = \begin{pmatrix} A & B \\ B & A \end{pmatrix} \cdot \begin{pmatrix} Q_{xx} + \frac{1}{3} S_{\text{vol}} \\ Q_{yy} + \frac{1}{3} S_{\text{vol}} \end{pmatrix} . \quad (\text{A15})$$

Now we change the variables to the deviations of Q_{xx} and Q_{yy} from the volume solutions,

$$\begin{pmatrix} \delta Q''_{xx} \\ \delta Q''_{yy} \end{pmatrix} = \begin{pmatrix} A & B \\ B & A \end{pmatrix} \cdot \begin{pmatrix} \delta Q_{xx} \\ \delta Q_{yy} \end{pmatrix}. \quad (\text{A16})$$

By determining the eigenvalues and eigenvectors of the coefficient matrix, it can be expressed by its diagonalized form and the corresponding orthogonal transformations,

$$\begin{pmatrix} \delta Q''_{xx} \\ \delta Q''_{yy} \end{pmatrix} = \frac{1}{\sqrt{2}} \begin{pmatrix} 1 & 1 \\ -1 & 1 \end{pmatrix} \cdot \begin{pmatrix} A - B & 0 \\ 0 & A + B \end{pmatrix} \cdot \frac{1}{\sqrt{2}} \begin{pmatrix} 1 & -1 \\ 1 & 1 \end{pmatrix} \cdot \begin{pmatrix} \delta Q_{xx} \\ \delta Q_{yy} \end{pmatrix}. \quad (\text{A17})$$

Now the system can be decoupled by a similarity transformation. Keeping only the decaying modes, we arrive at the solution

$$\begin{pmatrix} \delta Q_{xx} \\ \delta Q_{yy} \end{pmatrix} = \frac{1}{\sqrt{2}} \begin{pmatrix} 1 & 1 \\ -1 & 1 \end{pmatrix} \cdot \begin{pmatrix} e^{-\sqrt{A-B}z} & 0 \\ 0 & e^{-\sqrt{A+B}z} \end{pmatrix} \cdot \frac{1}{\sqrt{2}} \begin{pmatrix} 1 & -1 \\ 1 & 1 \end{pmatrix} \cdot \begin{pmatrix} \alpha \\ \beta \end{pmatrix}. \quad (\text{A18})$$

The asymptotic Cauchy boundary conditions are obtained by differentiating the solutions by z , taken at infinity,

$$\begin{pmatrix} \delta Q'_{xx} \\ \delta Q'_{yy} \end{pmatrix} = -\frac{1}{\sqrt{2}} \begin{pmatrix} 1 & 1 \\ -1 & 1 \end{pmatrix} \cdot \begin{pmatrix} \sqrt{A-B} & 0 \\ 0 & \sqrt{A+B} \end{pmatrix} \cdot \frac{1}{\sqrt{2}} \begin{pmatrix} 1 & -1 \\ 1 & 1 \end{pmatrix} \cdot \begin{pmatrix} \delta Q_{xx} \\ \delta Q_{yy} \end{pmatrix}. \quad (\text{A19})$$

The explicit boundary conditions for Q_{xx} and Q_{yy} then are

$$\begin{aligned} Q'_{xx}(z = \infty) &= -\frac{1}{2} \left(\sqrt{A+B} + \sqrt{A-B} \right) \cdot \left(Q_{xx} + \frac{1}{3} S_{\text{vol}} \right) \\ &\quad -\frac{1}{2} \left(\sqrt{A+B} - \sqrt{A-B} \right) \cdot \left(Q_{yy} + \frac{1}{3} S_{\text{vol}} \right), \end{aligned} \quad (\text{A20})$$

$$\begin{aligned} Q'_{yy}(z = \infty) &= -\frac{1}{2} \left(\sqrt{A+B} - \sqrt{A-B} \right) \cdot \left(Q_{xx} + \frac{1}{3} S_{\text{vol}} \right) \\ &\quad -\frac{1}{2} \left(\sqrt{A+B} + \sqrt{A-B} \right) \cdot \left(Q_{yy} + \frac{1}{3} S_{\text{vol}} \right). \end{aligned} \quad (\text{A21})$$

The remaining linearized Euler-Lagrange equations are already decoupled which immediately

yields the corresponding Cauchy boundary conditions at infinity,

$$Q'_{xy}(z = \infty) = -\sqrt{G_{33}} \cdot Q_{xy} , \quad (\text{A22})$$

$$Q'_{xz}(z = \infty) = -\sqrt{\frac{2G_{44}}{2 + k_{21} + k_{31}}} \cdot Q_{xz} , \quad (\text{A23})$$

$$Q'_{yz}(z = \infty) = -\sqrt{\frac{2G_{44}}{2 + k_{21} + k_{31}}} \cdot Q_{yz} , \quad (\text{A24})$$

$$\psi'(z = \infty) = -\sqrt{\frac{\tau}{\kappa}} \cdot \psi . \quad (\text{A25})$$

The Cauchy boundary condition at infinity has to be derived from variational calculus in order to be included into the relaxation. It is obtained from the bulk energy functional \mathcal{F} and a boundary energy functional \mathcal{F}_∞ ,

$$\frac{\partial \mathcal{F}_\infty}{\partial X} + \frac{\partial \mathcal{F}}{\partial X'} = 0 , \quad (X = \psi, Q_{ij}) . \quad (\text{A26})$$

To obtain this boundary energy functional we insert the Cauchy boundary conditions (A20)–(A25), previously derived from the linearized Euler-Lagrange equations, into the variational equation (A26). This immediately yields the six partial derivatives of the boundary energy functional,

$$\begin{pmatrix} \frac{\partial \mathcal{F}_\infty}{\partial Q_{xx}} \\ \frac{\partial \mathcal{F}_\infty}{\partial Q_{yy}} \end{pmatrix} = -\frac{1}{2} \begin{pmatrix} 2 + k_{21} + k_{31} & 1 + k_{21} + k_{31} \\ 1 + k_{21} + k_{31} & 2 + k_{21} + k_{31} \end{pmatrix} \cdot \begin{pmatrix} Q'_{xx} \\ Q'_{yy} \end{pmatrix} \quad (\text{A27})$$

$$= \frac{1}{4} \begin{pmatrix} 2 + k_{21} + k_{31} & 1 + k_{21} + k_{31} \\ 1 + k_{21} + k_{31} & 2 + k_{21} + k_{31} \end{pmatrix} \cdot \begin{pmatrix} \sqrt{A + B} + \sqrt{A - B} & \sqrt{A + B} - \sqrt{A - B} \\ \sqrt{A + B} - \sqrt{A - B} & \sqrt{A + B} + \sqrt{A - B} \end{pmatrix} . \quad (\text{A28})$$

$$\begin{pmatrix} Q_{xx} + \frac{1}{3} S_{\text{vol}} \\ Q_{yy} + \frac{1}{3} S_{\text{vol}} \end{pmatrix} = \begin{pmatrix} U & V \\ V & U \end{pmatrix} \cdot \begin{pmatrix} Q_{xx} + \frac{1}{3} S_{\text{vol}} \\ Q_{yy} + \frac{1}{3} S_{\text{vol}} \end{pmatrix} \quad (\text{A29})$$

$$\frac{\partial \mathcal{F}_\infty}{\partial Q_{xy}} = -Q'_{xy} = \sqrt{G_{33}} \cdot Q_{xy} \quad (\text{A30})$$

$$\frac{\partial \mathcal{F}_\infty}{\partial Q_{xz}} = -\frac{1}{2} (2 + k_{21} + k_{31}) Q'_{xz} = \sqrt{\frac{1}{2} (2 + k_{21} + k_{31}) G_{44}} \cdot Q_{xz} \quad (\text{A31})$$

$$\frac{\partial \mathcal{F}_\infty}{\partial Q_{yz}} = -\frac{1}{2} (2 + k_{21} + k_{31}) Q'_{yz} = \sqrt{\frac{1}{2} (2 + k_{21} + k_{31}) G_{44}} \cdot Q_{yz} \quad (\text{A32})$$

$$\frac{\partial \mathcal{F}_\infty}{\partial \psi} = -\kappa \psi' \quad (\text{A33})$$

$$= \sqrt{\kappa\tau} \cdot \psi \quad (\text{A34})$$

Now the boundary energy functional is obtained by integration, just in the same way a potential field is calculated from a given force field in classical mechanics. The final result, quoted in the main text, reads

$$\begin{aligned} \mathcal{F}_\infty = & \frac{1}{2} U (Q_{xx}^2 + Q_{yy}^2) + \frac{1}{3} (U + V) S_{\text{vol}} (Q_{xx} + Q_{yy}) \\ & + V Q_{xx} Q_{yy} + \frac{1}{2} \sqrt{G_{33}} \cdot Q_{xy}^2 \\ & + \frac{1}{2} \sqrt{\frac{1}{2} (2 + k_{21} + k_{31}) G_{44}} \cdot (Q_{xz}^2 + Q_{yz}^2) \\ & + \frac{1}{2} \sqrt{\kappa\tau} \cdot \psi^2. \end{aligned} \quad (\text{A35})$$

- [1] B. Jérôme, Rep. Prog. Phys. **54**, 391 (1991).
- [2] C. Oldano, G. Barbero, J. Phys. Lett. (Paris) **46**, 451 (1985).
- [3] G. Barbero, A. Sparavigna, A. Strigazzi, Nuovo Cimento D **12**, 1259 (1990).
- [4] A. Poniewierski, R. Holyst, Phys. Rev. A **38**, 3721 (1988).
- [5] X. Zhuang, L. Marrucci, Y.R. Shen, Phys. Rev. Lett. **73**, 1513 (1994).
- [6] J. Als-Nielsen, F. Christensen, P.S. Pershan, Phys. Rev. Lett. **48**, 1107 (1982).
- [7] G. Barbero, N.V. Madhusudana, C. Oldano, J. Phys. (Paris) **50**, 226 (1989).
- [8] G. Skačej, A. L. Alexe-Ionescu, G. Barbero, S. Žumer, Phys. Rev. E **57**, 1780 (1998).
- [9] V. Pergamenshchik, S. Žumer, Phys. Rev. E **59**, 2531 (1999).
- [10] G. Barbero, G. Skačej, A.L. Alexe-Ionescu, S. Žumer, Phys. Rev. E **60**, 628 (1999).
- [11] B. Tjipto-Margo, D.E. Sullivan J. Chem. Phys. **88**, 6620 (1988).
- [12] J. Stelzer, P. Galatola, G. Barbero, L. Longa, Phys. Rev. E **55**, 7085 (1997).
- [13] J. Stelzer, P. Galatola, G. Barbero, L. Longa, Phys. Rev. E **55**, 477 (1997).
- [14] E. Martin del Rio, M. M. Telo da Gama, E. de Miguel, L. F. Rull, Phys. Rev. E **52**, 5028 (1995).
- [15] W. L. McMillan, Phys. Rev. A **6**, 936 (1972); Phys. Rev. A **7**, 1673 (1973).
- [16] P. Galatola, M. Źelazna, I. Lelidis, Eur. Phys. J B **2**, 51 (1998).

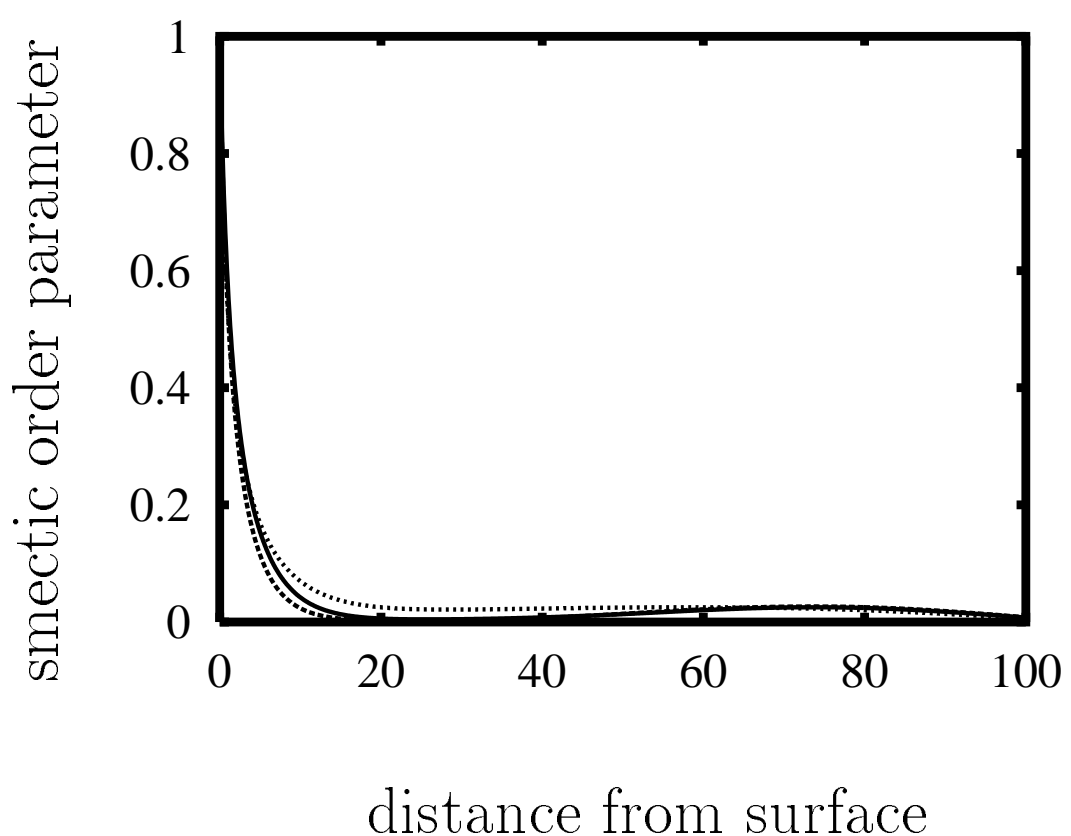
FIG. 1: Profile of the smectic order parameter $\psi(z)$ for reduced temperature $t = 0.0$, at various intrinsic smectic wave numbers q_0 . Solid line: $\psi(z)$ at $q_0 = 0.3$; dashed line: $\psi(z)$ at $q_0 = 0.6$; dotted line: $\psi(z)$ at $q_0 = 0.8$.

FIG. 2: Profile of the nematic order parameters $S(z)$ and $T(z)$ for uniaxial and biaxial order, respectively, for reduced temperature $t = 0.0$, at various intrinsic smectic wave numbers q_0 . Solid line: $S(z)$ at $q_0 = 0.3$; dashed line: $S(z)$ at $q_0 = 0.6$; upper dotted line: $S(z)$ at $q_0 = 0.8$; lower dotted line: $T(z)$ at $q_0 = 0.8$.

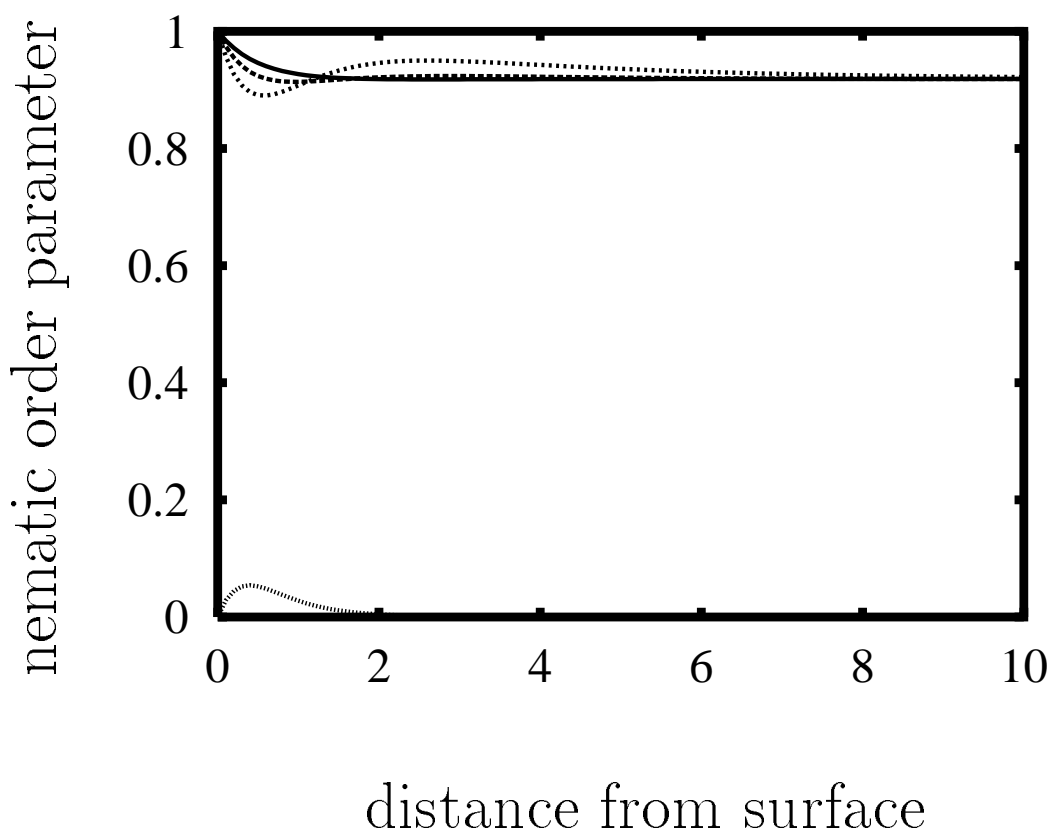
FIG. 4: Profile of the director tilt angle $\Theta(z)$ for reduced temperature $t = 1.0$, at various intrinsic smectic wave numbers q_0 . Solid line: $\Theta(z)$ at $q_0 = 0.3$; dashed line: $\Theta(z)$ at $q_0 = 0.6$; dotted line: $\Theta(z)$ at $q_0 = 0.8$.

FIG. 3: Profile of the director tilt angle $\Theta(z)$ for reduced temperature $t = 0.0$, at various intrinsic smectic wave numbers q_0 . Solid line: $\Theta(z)$ at $q_0 = 0.3$; dashed line: $\Theta(z)$ at $q_0 = 0.6$; dotted line: $\Theta(z)$ at $q_0 = 0.8$.

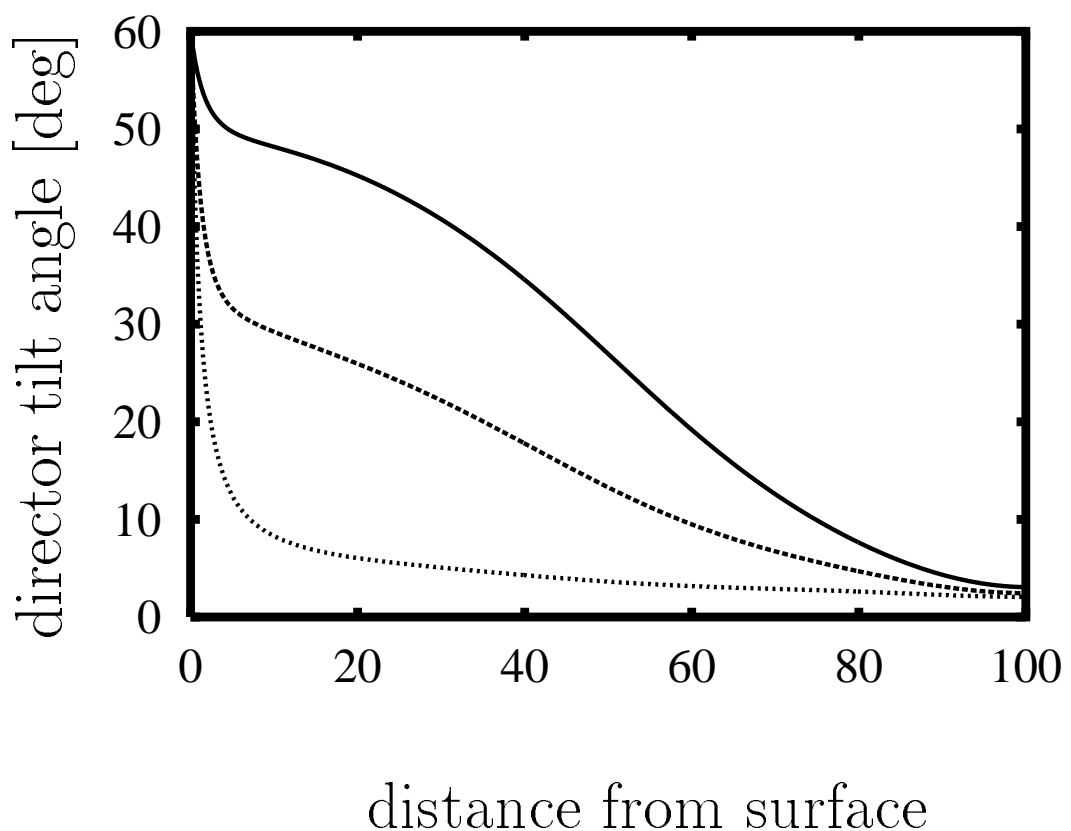
J. Stelzer and R. Bernhard : Figure 1



J. Stelzer and R. Bernhard : Figure 2



J. Stelzer and R. Bernhard : Figure 3



J. Stelzer and R. Bernhard : Figure 4

